

Investigation of the Chill Down Process in the LUMEN LOX/LNG Demonstrator Engine

By Sebastian KLEIN,¹⁾ Dmitry SUSLOV,¹⁾ Anirudh MUKUND SARAF,¹⁾ Michael BÖRNER,¹⁾ Robson DOS SANTOS HAHN,¹⁾ Kai DRESIA,¹⁾ Wolfgang ARMBRUSTER,¹⁾ Christopher GROLL,¹⁾ Tobias TRAUDT,¹⁾ Justin HARDI,¹⁾ and Jan DEEKEN¹⁾

¹⁾DLR Institute of Space Propulsion, DLR, Lampoldshausen, Germany

(Received May 28th, 2023)

The DLR project LUMEN (Liquid upper stage demonstrator engine) aims at developing a modular LOX/LNG bread-board engine in the 25 kN thrust class for operation at the new P8.3 test facility in Lampoldshausen. To ensure an easy exchange of components, they were arranged in the test cell with significant spacing between them. In addition, a large number of control valves have been installed, allowing new approaches to be investigated for controlling the system. As these design decisions increase the heat capacity of the demonstrator engine supply system, a detailed understanding of the chill down process is of great interest. An adequate chill down is essential for reliable engine operation as two-phase flow within the feed system can negatively impact both pump operation and combustion stability. Component tests of the oxygen turbo pump (OTP) and the thrust chamber assembly (TCA) have been performed as steps toward testing the fully integrated LUMEN engine. Experimental chill down data from these campaigns is analysed to evaluate the flow conditions at ignition. The results will then be used to develop an optimised cooling sequence that will significantly improve the chill down process.

Key Words: expander-bleed cycle, LUMEN, LOX/LNG, chill down, two-phase flow

Nomenclature

d_i	: Inner diameter, mm
e	: Wall thickness, mm
f_s	: Sampling frequency, Hz
LH2	: Liquid hydrogen
LNG	: Liquefied natural gas
LOX	: Liquid oxygen
l	: Length, m
P	: Pressure, bar
\dot{q}	: Heat flux, W/m ²
ROF	: Mixture ratio, -
T	: Temperature, K
t	: Time, s
ρ	: Density, kg/m ³
χ	: void fraction, -

Subscripts

CC	: Combustion chamber
CHF	: Critical heat flux
g	: Gaseous
in	: inlet
l	: Liquid
Leid	: Leidenfrost point
m	: Mixture
norm	: normalised
out	: outlet
sat	: Saturation
st	: Structure
W	: Wall

1. Introduction

Cryogenic rocket engines, powered by cold propellants such as liquefied natural gas (LNG) and liquid oxygen (LOX), are

widely used in space transportation due to their high energy density compared to storable non-cryogenic propellants. However, their operation requires a critical process known as the chill down, which includes cooling the engine components to their operating temperature before startup. The cryogenic liquids are routed from their respective storage tanks toward the combustion chamber. Prior to chill down, lines and engine are in thermal equilibrium with the surrounding environment. When these components are purged with cryogenic fluids, the heat stored in the structure is transferred to the fluid which causes it to evaporate.¹⁾ Once sufficient heat has dissipated from the structure, a steady liquid mass flow commences, signifying the completion of the chill down process. The duration and specific procedure for chill down vary depending on the engine's design, size, and operating conditions. Properly executing the chill down process is crucial to ensure a vapor-free inlet flow for the pumps and predictable engine startup. The chill down process was studied by several groups in the past. The utilization of cryogenic upper stage engines, such as the RL10, requires thermal preconditioning of the turbopumps before operation.²⁾ This process is divided into two stages. Initially, the engine undergoes cooling at the launch pad using liquid helium before liftoff. The chill down at the launch pad requires additional equipment on the launch pad but reduces the required mass flow in the second phase. However, the structure heats up again during operation of the main stage. Subsequently, shortly after liftoff, oxygen is released through the LOX pump into the combustion chamber and vented off board. On the liquid hydrogen (LH2) side, the propellant is led through the LH2 pump and then expelled to the exterior via vent valves.

A passive recirculation approach in the LOX system was presented by Li et al.³⁾ They used the natural convective forces to maintain the recirculation of the cryogenic propellant.

Their findings were that this method is highly susceptible to flow instabilities. In addition, the effects of subcooled LOX were investigated. It was found that lower structural temperatures can be achieved at the cost of higher flow instabilities.

The LUMEN engine is a modular, LOX/LNG, research platform, which will be operated at the P8.3 test facility.⁴⁾ To maximize the versatility of the research engine, the main components were strategically positioned with adequate spacing within the test cell. This arrangement facilitates accessibility for maintenance and adjustment purposes. Additionally, a considerable number of control valves have been integrated to enable the operation of the engine across a wide range of operating conditions while also allowing for tests of novel control and monitoring strategies. Consequently, these design choices result in a high structural mass, mainly due to the valves, and a large surface area, due to the long pipes.

In this paper the chill down process of the components tests of the LOX turbo pump (OTP) and the thrust chamber assembly (TCA) are evaluated in terms of cooling capacity and whether a reduction in the total amount of fluid required is possible. First, the theoretical foundations of the cryogenic chill down will be described. Then, a brief overview of the LUMEN research engine is given, followed by a description of the setups used. The main part of this paper consists of the presentation of the measurements during the chill down process. Finally, the cooling process is evaluated with an optimized cooling sequence based on the previously obtained results.

2. Cryogenic chill down

The chill down of a cryogenic system is a complex process, since it involves unsteady two-phase heat and mass transfer.⁵⁾ This process can be described by the reverse boiling curve,¹⁾ which is given in Fig. 1. The heat flux from the wall into the fluid \dot{q} is plotted against the walls degree of superheating $\Delta T = T_W - T_{sat}$. The chill down process is a temperature-controlled process, where the heat flux \dot{q} is a function of the temperature difference ΔT . This forces the route in Fig. 1 to follow $D \rightarrow C \rightarrow B \rightarrow A$.⁵⁾

Depending on this temperature difference, a different boiling regime sets in. During the chill down process, first film boiling occurs. The temperature and the heat flux are decreasing until the Leidenfrost point (C) is reached. Here the flow regime changes to transition boiling, which is accompanied by an increasing heat flux as the temperature decreases. The critical heat flux \dot{q}_{CHF} is reached at point B, then the heat flux is decreasing until reaching the onset of nucleate boiling (ONB) and a single phase flow is formed.

The void fraction χ is given by

$$\chi = V_g/V_m \quad (1)$$

with

$$V_m = V_g + V_l \quad (2)$$

where V_g and V_l are the volumes of the gas, respectively the liquid phase and V_m is the total volume of the mixture. Knowing the void fraction, the effective mixtures density ρ_m can be

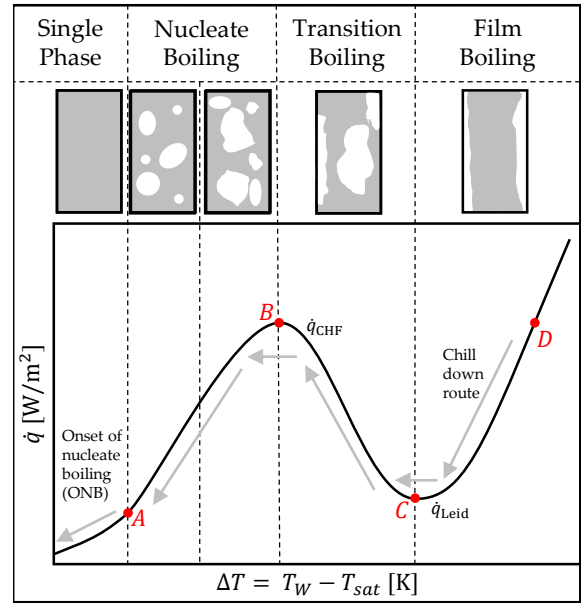


Fig. 1. Typical boiling curve, adapted from Reference,⁵⁾ grey represents the liquid phase, white represents the gaseous phase.

calculated as a function of the density of the liquid phase ρ_l and the gaseous phase ρ_g .⁶⁾

$$\rho_m = (1 - \chi)\rho_l + \chi\rho_g \quad (3)$$

3. Engine architecture

LUMEN is operated in the expander bleed cycle and will have a large throttling range around the nominal operational point of combustion chamber pressure $P_{CC} = 60$ bar and a mixture ratio of $ROF = 3.4$.⁴⁾

A schematic indicating the main components and valves is given in Fig. 2.

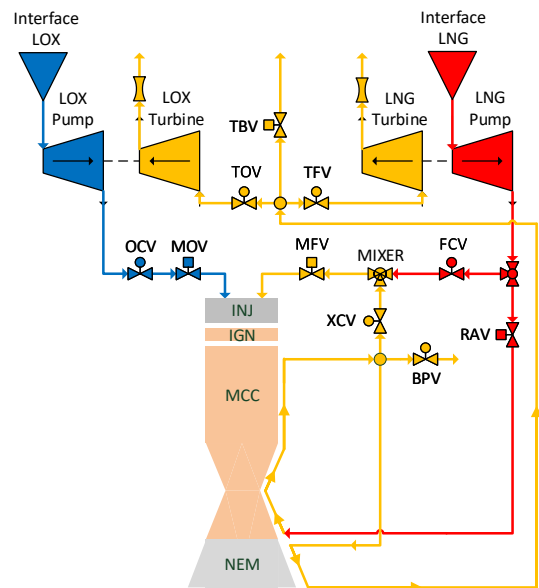


Fig. 2. Schematic representation of the LUMEN demonstrator architecture

The engine is powered by two separated turbo pumps, which are

both driven by the heated cooling channel mass flow. In total 6 control valves (OCV, XCV, FCV, BPV, TOV, TFV) and 4 shutoff valves (MOV, MFV, RAV, TBV) are in use. The valve labelled TBV is a normally closed emergency shutoff valve, which acts as a bypass to the turbines if load needs to be shed rapidly. The fuel mass flow is split by means of FCV and RAV. The mass flow set by the FCV is fed directly to the injector head (INJ). The main combustion chamber (MCC) is cooled by the methane mass flow set by RAV. After exiting the cooling channels this mass flow is again split. Part of it is routed through the nozzle extension (NEM), providing gaseous methane to the turbines. The remaining methane passes the XCV to be introduced to the mixer and recombined with colder liquid, as set by the FCV, in order to define the methane temperature in the injector head. In order to achieve good accessibility and interchangeability of the components, they have been installed in the test cell with the necessary spacing. This results in long pipes between the components. Thereby and through the number and the mass of the valves, the total mass of the engine is significant higher than a flight configuration.

On the pump side, previous work focused on the thermal design of the oxygen pump,⁷⁾ the use of a tangential injection device to reduce cavitation at the leading edge of the inducer blade of the fuel pump.⁸⁾ On the combustor side, the design of the regenerative cooling system was reviewed⁹⁾ and the flame anchoring for shear coaxial injectors was studied.¹⁰⁾ As the flame anchoring affects the heat flow from the combustion chamber to the cooling channels, it has a huge impact on engine performance. Beside the component research, a closed-loop control was established by combining machine learning with a transient simulation environment.¹¹⁾

4. Experimental setup

Two experimental setups were utilized to study the chill down behaviour, namely the OTP and TCA configurations. In the TCA configuration, the combustion chamber was used with piping but without the turbo pumps. On the other hand, in the OTP configuration, only the turbo pump together with the supply line were operated. As the position of the LNG and LOX interfaces are mirrored in both test cells, different supply lines were used.

4.1. OTP setup

The relevant part of the experimental setup for this paper is given in Fig. 3 The oxygen turbo pump is connected to the test bench interface via the oxygen supply line. The supply line has a length of $l_{OTP,LOX} \approx 2.5$ m. The inner diameter is $d_i = 53$ mm and the wall thickness is $e = 2$ mm. To determine the mass flow \dot{m}_{LOX} , the turbine flow meter in the test bench is polled at a sampling rate of $f_s = 10$ Hz. The fluid temperatures are measured at the test bench interface ($T_{LOX, bench}$), as well as in the pump inlet ($T_{LOX, in}$) and outlet ($T_{LOX, out}$). In addition the structural temperatures of the pump are measured at six locations, as indicated in Fig 4. Three measuring positions are distributed over the circumference of the inlet flange ($T_{st, in1} - T_{st, in3}$) and three are placed in circumferential direction in the volute ($T_{st, vo1} - T_{st, vo3}$). The measuring points in the component are countersunk, with

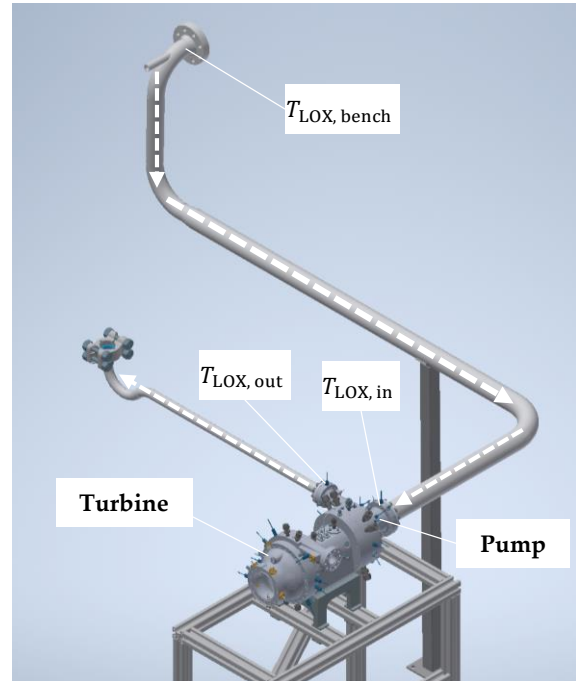


Fig. 3. OTP setup: Lox feed line with turbo pump

a wall thickness of 1 mm in front of each measuring point. The inlet measurement positions are integrated into the flange that connects the pump to the supply line. The temperature sensors have a sample rate of $f_s = 100$ Hz.

The chill down analysis of the OTP-campaign focuses solely on the inlet of the pump, which is the most critical part due to low static pressure and high relative speeds of the impeller blades. The analysis does not consider the piping system downstream of the pump. A comparison of the pump and supply line geometries reveals that they have similar masses. However, the pump has significantly less surface area in contact with the environment and the internal fluid compared to the supply line. As a result, it takes much more effort to cool the pump to operating temperature.

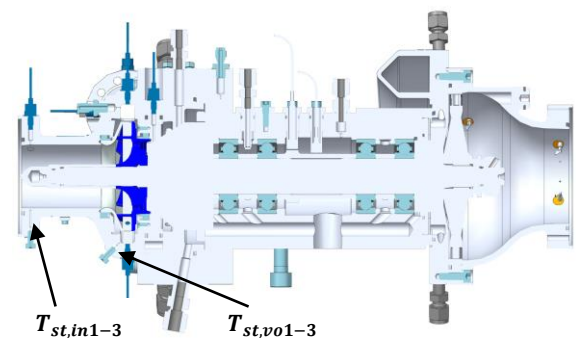


Fig. 4. Oxygen turbopump: Structural temperature sensor positions⁴⁾

4.2. TCA setup

The LOX supply line is shown in Fig. 5 and marked with arrows. The LNG piping can be seen on the left, but will not be discussed in detail as it is beyond the scope of this paper. The supply line has a length of $l_{TCA,LOX} \approx 3.3$ m, with an inner diameter of $d_i = 24$ mm and a wall thickness of $e = 2$ mm. In this setup, liquid is provided by a high pressure supply system

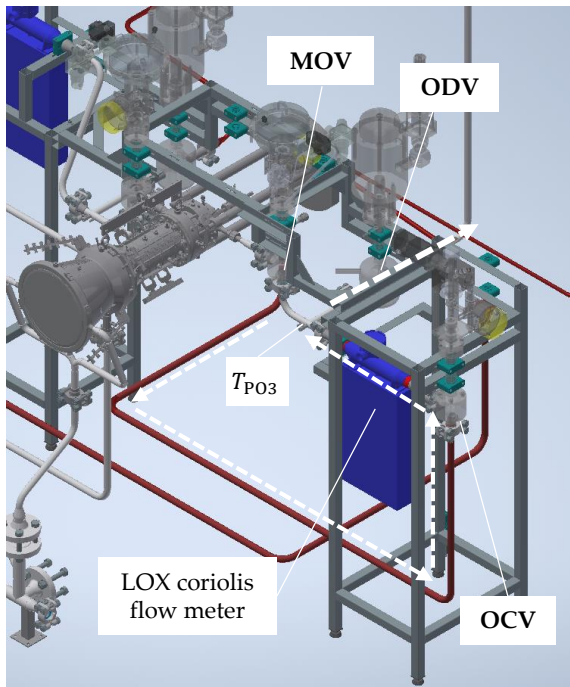


Fig. 5. TCA setup: LOX

on the bench side, therefore the supply line can be smaller in comparison to the supply line utilized in the OTP setup.

In this study, the fluid temperatures were measured at the interface of the test bench ($T_{\text{LOX, bench}}$) and at the tee in the line using a thermocouple type K class 3 at $f_s = 100\text{ Hz}$. The LOX mass flow was measured at the interface of the test bench using a turbine flow meter at $f_s = 1\text{ kHz}$. The density of the fluid was directly measured using the coriolis mass flow meter at $f_s = 1\text{ kHz}$. The oxygen dump valve (ODV) is open during the chill down process, while the main oxygen valve (MOV) remains closed.

5. Results

The following is a discussion of the experimental results of the three test cases (A, B, C). The setups used are given in Table 1.

Table 1. Setups used for the test cases

Case	Setup
A	OTP
B	TCA
C	TCA

First, the chill down sequences of test cases A and B are described. The chill down sequence of test C, which is presented at the end, is based on the experience gained from these tests.

5.1. Case A

The main goal of the OTP-campaign chill down analysis was to find out if the pump, especially its inlet, was cooled down adequately. To do so, the main measurements are given in the following. The mass flow during the chill down process can be found in Fig. 6. At the beginning ($-8 < t_{\text{norm}} < -6$), strong fluctuations in the mass flow can be observed, which are followed by a phase of low mass flow at $t_{\text{norm}} = -5.5$. Finally, the

mass flow settles to a constant value at $t_{\text{norm}} = -4$ until the chill down sequence is finished at $t_{\text{norm}} = 0$. The structural tempera-

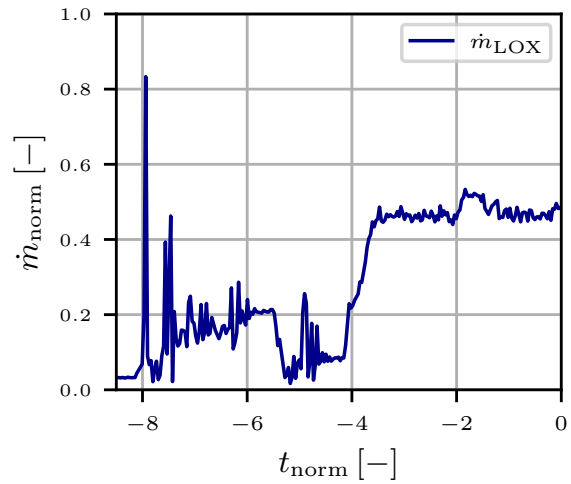


Fig. 6. Mass flow during the chill down

tures of the LOX pump and the corresponding time derivatives are shown in Fig. 7 respectively Fig. 8 and the fluid temperatures are shown in Fig. 9. The temperature curves shown in Fig. 7 are the mean temperatures measured by the three thermocouples distributed over the circumference of the pump inlet flange

$$T_{\text{st, in}} = (T_{\text{st, in1}} + T_{\text{st, in2}} + T_{\text{st, in3}})/3 \quad (4)$$

respectively, in the volute:

$$T_{\text{st, vo}} = (T_{\text{st, vo1}} + T_{\text{st, vo2}} + T_{\text{st, vo3}})/3 \quad (5)$$

The individual measurements are shown additionally as dotted lines. The structure of the pump cools heterogeneously. Although the pump volute is downstream of the inlet, the temperature decreases here more rapidly than at the inlet. This may be explained by either of two effect.

Firstly, the direction of the flow, which is parallel to the pipe wall at the inlet, but in a radial direction in the volute. The change in direction in the pump also creates a more complex flow field, including turbulence, which increases the heat transfer between the fluid and the structure.

Secondly, the wall thickness in the volute is much lower than at the inlet. A flange is used to connect the pump to the supply line (see Fig. 4); in this position, both the local wall thickness and the associated heat capacity of the structure are significantly increased.

By deriving the structural temperatures $T_{\text{st, in}}$ and $T_{\text{st, vo}}$ according to time, it is possible to analyse the transient behaviour of the chill down process in detail. Particularly large temperature drops, which indicate a change of the two-phase flow regime, are easy to identify. Transition boiling in the volute is reached at $t_{\text{norm}} = -6$, while it is reached at the inlet at $t_{\text{norm}} = -3.5$. The effects of the higher heat flux due to transition boiling can also be seen in the fluid temperature, as indicated by fluid measurements taken at the pump inlet, outlet and test bench interface, as plotted in Fig. 9.

The temperature at the test bench interface is $T_{\text{LOX, bench}} = 110\text{ K}$ at the beginning and its cooled down in the first interval of

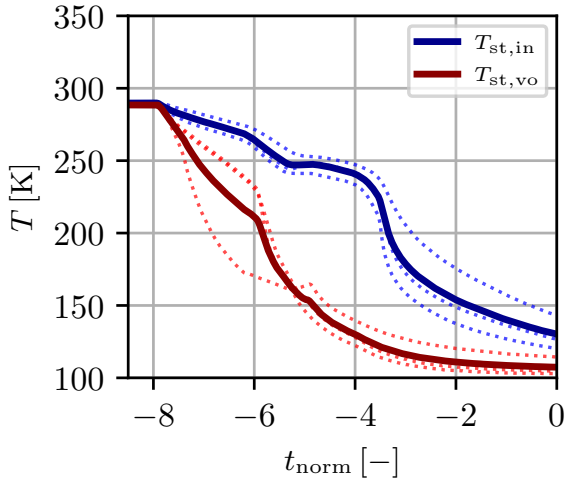


Fig. 7. Structural temperatures of the LOX-pump

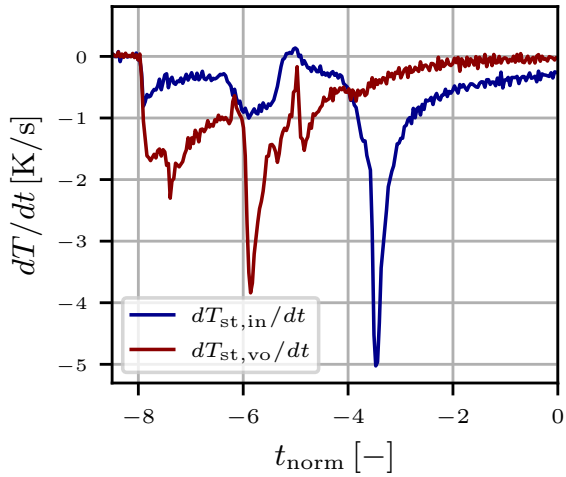


Fig. 8. Temporal derivative of the structural temperature of the LOX-pump

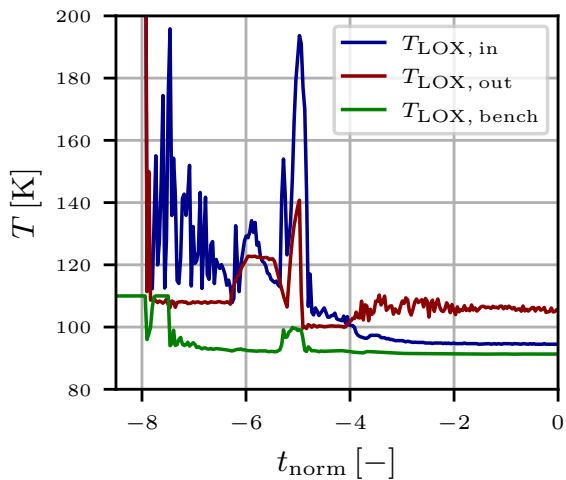


Fig. 9. Fluid temperature of the OTP-campaign

the chill down process ($-8 < t_{\text{norm}} < -7$). Apart from a short duration temperature rise at $t_{\text{norm}} = -5$, what coincides with the low mass flow at this time, $T_{\text{LOX,bench}}$ is nearly constant.

The fluids temperature at the pump inlet and outlet, $T_{\text{LOX,in}}$ and $T_{\text{LOX,out}}$, differ significantly from each other during the chill down process. While $T_{\text{LOX,in}}$ is extremely unstable until $t_{\text{norm}} = -6$, the outlet temperature drops abruptly to a stable value of $T_{\text{LOX,out}} = 110$ K. During the period $-6 < t_{\text{norm}} < -5$ in which the two-phase flow regime transition in the volute takes place, the fluids temperature in the pump rises due to the higher heat flux from the structure into the fluid. This heating reaches its maximum at $t_{\text{norm}} = -5$, here temperature values at the inlet of $T_{\text{LOX,in}} = 190$ K are reached. At the same time high fluctuations of the mass flow \dot{m}_{LOX} can be observed. After $t_{\text{norm}} = -5$ the fluid temperatures stabilize and reach constant values of $T_{\text{LOX,in}} = 95$ K and $T_{\text{LOX,out}} = 105$ K. In steady state the temperature rise over the supply line is $\Delta T_{\text{line}} = 3$ K and over the pump $\Delta T_{\text{pump}} = 12$ K.

The results show that the chill down procedure used adequately chilled down the pump. Stable temperature conditions of the fluid are reached at $t_{\text{norm}} = -2$ and the region of two-phase flow regime transition have already been passed through. Therefore the chill down procedure could be shortened to this point in time. However, it should be noted that the structural temperature at the inlet lags behind the fluid temperature due to the thermal capacity of the massive flange and that this region is the most critical region in terms of the occurrence of cavitation. It is suspected that the flange used creates a high local heat input, it is recommended to move the flange away from the impeller inlet.

5.2. Case B

The following is a description of the chill down prior to ignition at $t_{\text{norm}} = 0$ of the LOX feed line in case B.

The mass flow \dot{m}_{LOX} , the temperatures at the interface T_{int} and in the line T_{PO3} , the density ρ_{LOX} and the void fraction χ_{LOX} of the LOX feed line during chill down are given in Fig. 10. The void fraction χ_{LOX} is calculated using equation 1, where ρ_l and ρ_g are calculated using the temperature measurement and ρ_m is measured directly via the coriolis flow meter. The chill down sequence starts at $t_{\text{norm}} = -0.9$ with a constant mass flow of $\dot{m}_{\text{norm}} = 0.2$. At $t_{\text{norm}} = -0.5$, the mass flow is quintupled until it is finally set to a low value of $\dot{m}_{\text{norm}} = 0.1$ at $t_{\text{norm}} = -0.2$, where it remains until ignition. The corresponding fluid temperatures in the line (T_{PO3}) and the interface of the test bench are decreasing abruptly with the beginning of the chill down sequence $t_{\text{norm}} = -0.9$. During this temperature drop, a local temperature rise can be observed at the P8 Interface, which is in line with the theory presented in Fig. 1. With respect to the density ρ_{LOX} , a steady flow is achieved between $t_{\text{norm}} = -0.65$ and $t_{\text{norm}} = -0.5$. During this period a density of $\rho_{\text{LOX}} = 660$ kg/m³ is measured, which indicates a void fraction of $\chi_{\text{LOX}} = 0.23$ by using equation 3. Then the mass flow is increased, which leads to a transient flow after $t_{\text{norm}} = -0.5$. The LOX temperature at the interface is decreasing towards $T_{\text{int}} = 104$ K, while the fluid temperature in the line increases by $\Delta T = 10$ K to $T_{\text{PO3}} = 143$ K. This heating is caused by an increasing heat flux from the structure towards the fluid, triggered by a change in the two phase flow regime.

After this highly transient region is left behind a steady state is formed at $t_{\text{norm}} = -0.34$, which can be identified by the density

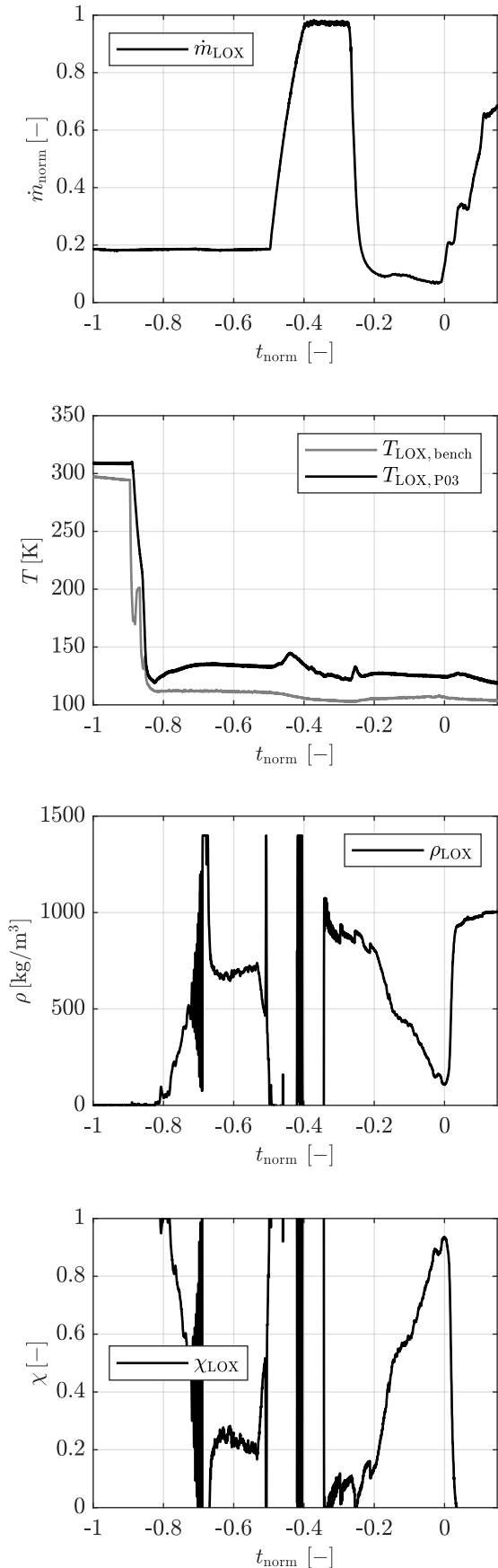


Fig. 10. Case B: TCA setup: LOX parameters)

measurement. The void fraction in this area is relatively low $\chi_{\text{LOX}} < 0.1$, hence the flow is nearly all liquid. Shortly before ignition ($t_{\text{norm}} = -0.28$), the mass flow is lowered. In the following χ_{LOX} is increasing over time, leading to a nearly complete gaseous flow at ignition. The explanation for this behavior is that, even the temperature and density measurement indicated a steady liquid flow, the structure is not completely cooled down. This leads to evaporation of the oxygen in the pipeline during the final process of the chill down. In summary, the chill down time must be extended in order to be able to enter the LOX injection head with a pure liquid phase when the engine starts.

5.3. Case C

When operating the entire engine, chill down requirements by pumps and TCA need to be combined. For the LOX pump it has to be ensured that liquid flow occurs as the pumps start in order to avoid blockage and possible pump stall. In the TCA setup, where no pump is utilized, achieving an adequate chill-down is attained by ensuring that the oxygen entering the injector head is in a pure liquid phase at the moment the main oxygen valves open. The deviation from this requirement observed in Case B necessitated changes to the chill down sequence. To this end the chill down time of the TCA was approximately doubled, which is still shorter than the chill down time found to be adequate in case A. The chill down time is limited by a desire to conserve LOX during this phase of engine operation.

The results of the chill down sequence of case C are given analogue to Fig. 10 in Fig. 11. The sequence starts with a very low gaseous mass flow, until $t_{\text{norm}} = -1.75$. During this period the fluid temperature in the line is abruptly decreasing, followed by a temporary heating until $t_{\text{norm}} = -1.75$. Like in the test cases described before, this transient behavior is an indication of a two-phase flow regime change, from film boiling to transition-, and nucleate boiling until a single phase liquid flow is achieved. This agrees with the density measurement and the resulting void fraction χ . In the moment the heating stops and the mass flow is increasing, the void fraction is decreasing from $\chi \approx 1$ to $\chi \approx 0$. The fact that values of $\chi < 0$ are obtained for the void fraction can be explained by the measurement error of the density and temperature measurement. In case A χ was decreasing before ignition, due to the heat stored in the structure, the mass flow was not decreased before ignition, but increased for a short period of time.

The results of the optimized chill down procedure look promising, since the fluids temperature in the line T_{P03} and χ are nearly constant for $t_{\text{norm}} > -1.5$. It can be assumed that liquid oxygen flows into the injector head when the engine is started.

6. Conclusion

In conclusion, this paper investigated the chill-down procedure of the LOX supply lines and the LOX pump in the LUMEN engine. Two cases using the TCA setup and one case using the OTP setup were analysed:

In case A (OTP setup), it was found that the chill-down of the pump was sufficient but the the structure cools down heterogeneously. Especially the inlet of the of the inducer, which is the most critical part in terms of chill down, cools down slower in

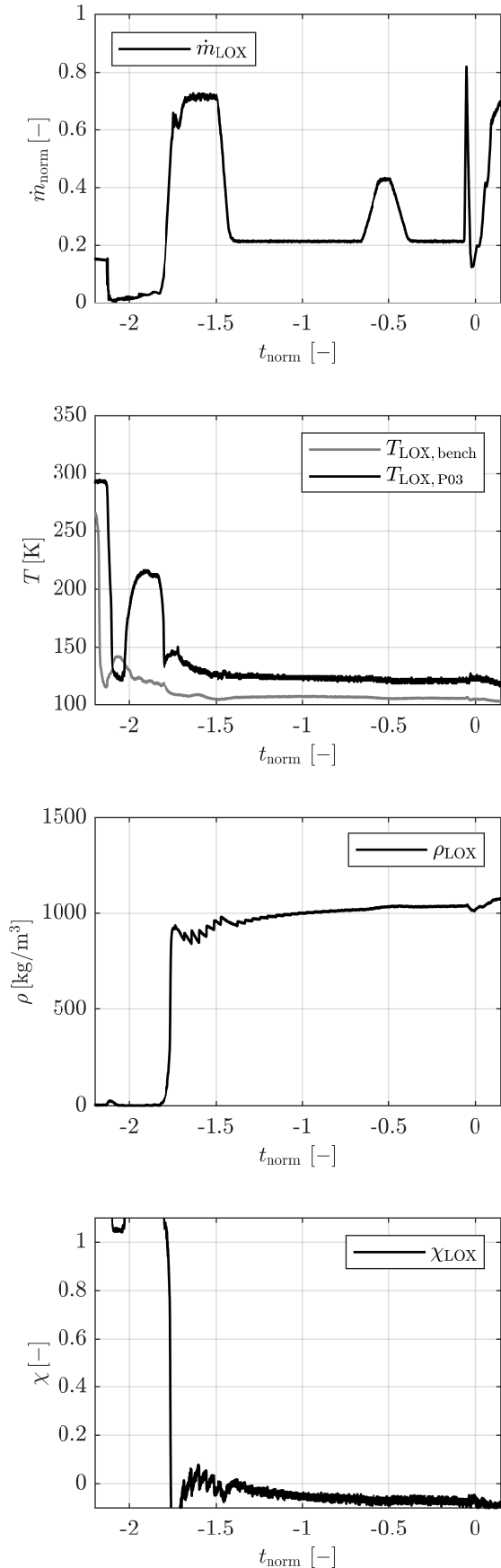


Fig. 11. Case C: TCA setup: LOX parameters)

comparison to the volute. The flange used at the inlet could be partly responsible for this behavior. In case B (TCA setup), it was determined that the chill-down of the supply line was inadequate, due to gaseous flow during ignition. In case C (TCA setup), an optimized (extended) chill-down sequence derived from the findings in case B was implemented. The changes had a positive impact as the cooling was sufficient, and the injector head was supplied with liquid oxygen during engine startup. The cooling sequences for the LOX side were determined and evaluated for both configurations, and they will be used in future test campaigns to ensure a smooth engine start. Since cooling down the pump takes much longer and requires more LOX, the cooling sequence in the final engine configuration is designed accordingly. Future work includes revising the pump's flange design to improve cooling at the impeller inlet, thereby enhancing overall engine performance and efficiency during startup.

Acknowledgments

The authors greatly acknowledge the support of the DLR P8 test facility team, Alex Grebe and Michael Andrick during the test campaigns.

References

- Darr, S. R., Hu, H., Shaeffer, R., Chung, J., Hartwig, J. W., Majumdar, A. K. (2015). Numerical simulation of the liquid nitrogen chilldown of a vertical tube. In 53rd aiaa aerospace sciences meeting (p. 0468).
- Santiago, J. (1996, July). Evolution of the RL10 liquid rocket engine for a new upperstage application. In 32nd Joint Propulsion Conference and Exhibit (p. 3013).
- Li, C., Zhuang, Y., Li, Y., Cheng, Y., Chen, E. (2019). Thermal behavior and flow instabilities during transient chilldown of liquid rocket engine by passive recirculation approach. *Cryogenics*, 99, 87-98.
- Traudt, T., Börner, M., Suslov, D., Dos Santos Hahn, R. H., Saraf, A. M., Klein, S., Deeken, J., Hardi, J., Oswald, M., Schlechtriem, S. Liquid Upper Stage Demonstrator Engine (LUMEN): Component Test Results and Project Progress. 73rd International Astronautical Congress, 18. - 22. Sep. 2022, Paris, France
- Hu, H., Xu, C., Zhao, Y., Ziegler, K. J., Chung, J. N. (2017). Boiling and quenching heat transfer advancement by nanoscale surface modification. *Scientific reports*, 7(1), 1-16.
- Wilson, P. S., Roy, R. A. (2008). An audible demonstration of the speed of sound in bubbly liquids. *American Journal of Physics*, 76(10), 975-981.
- Saraf, A. M., Traudt, T., Oswald, M. (2021, May). LUMEN Turbopump: Preliminary Thermal Model. In *Journal of Physics: Conference Series* (Vol. 1909, No. 1, p. 012052). IOP Publishing.
- Groll, C., Traudt, T., Oswald, M., Schlechtriem, S. (2022). Inducer Cavitation Control via Inlet Swirl. 33rd International Symposium on Space Technology and Science, 2022
- Haemisch, J., Suslov, D., Waxenegger-Wilfing, G., Dresia, K., Oswald, M. (2021). LUMEN-Design of the Regenerative Cooling System for an Expander Bleed Cycle Engine Using Methane. 7th International Space Propulsion Conference, 17.-19. Mar. 2021, virtual.
- Börner, M., Martin, J., Hardi, J., Suslov, D., Deeken, J. C., Oswald, M. (2021). Lumen thrust chamber-flame anchoring for shear coaxial injectors. 7th International Space Propulsion Conference, 17.-19. Mar. 2021, virtual.
- Dresia, K., Waxenegger-Wilfing, G., Dos Santos Hahn, R. H., Deeken, J. C., Oswald, M. (2021). Nonlinear control of an expander-bleed rocket engine using reinforcement learning. 7th International Space Propulsion Conference, 17.-19. Mar. 2021, virtual.